



HAL
open science

Chemically Amplified Photoresists for 193-Nm Photolithography: Effect of Molecular Structure and Photonic Parameters on Photopatterning

Hassan Ridaoui, Ali Dirani, Olivier Soppera, Esma Ismailova, Cyril Brochon,
Guy Schlatter, Georges Hadziioannou, Raluca Tiron, Philippe Bandelier,
Claire Sourd

► **To cite this version:**

Hassan Ridaoui, Ali Dirani, Olivier Soppera, Esma Ismailova, Cyril Brochon, et al.. Chemically Amplified Photoresists for 193-Nm Photolithography: Effect of Molecular Structure and Photonic Parameters on Photopatterning. *Journal of Polymer Science Part A: Polymer Chemistry*, 2010, 48 (6), pp.1271-1277. 10.1002/pola.23866 . hal-00679919

HAL Id: hal-00679919

<https://hal.science/hal-00679919v1>

Submitted on 28 Sep 2024

HAL is a multi-disciplinary open access archive for the deposit and dissemination of scientific research documents, whether they are published or not. The documents may come from teaching and research institutions in France or abroad, or from public or private research centers.

L'archive ouverte pluridisciplinaire **HAL**, est destinée au dépôt et à la diffusion de documents scientifiques de niveau recherche, publiés ou non, émanant des établissements d'enseignement et de recherche français ou étrangers, des laboratoires publics ou privés.



Distributed under a Creative Commons Attribution - NonCommercial 4.0 International License

Chemically Amplified Photoresists for 193-Nm Photolithography: Effect of Molecular Structure and Photonic Parameters on Photopatterning

Hassan Ridaoui¹, Ali Dirani¹, Olivier Soppera¹, Esma Ismailova², Cyril Brochon³, Guy Schlatter², Georges Hadziioannou³, Raluca Tiron⁴, Philippe Bandelier⁴, Claire Sourd⁴

¹Département de Photochimie Générale, CNRS – FRE 3252, Université de Haute Alsace, Mulhouse, France

²Laboratoire d'Ingénierie des Polymères pour les Hautes Technologies, EAC 4379, Université de Strasbourg, Ecole Européenne de Chimie, Polymères et Matériaux, Strasbourg, France

³Laboratoire de Chimie des Polymères Organiques (LCPO) - UMR5629, Université Bordeaux 1/Institut Polytechnique de Bordeaux, Talence, France

⁴CEA-LETI, MINATEC, Grenoble, France

ABSTRACT: Next generations of microelectronic devices request further miniaturized systems. In this context, photolithography is a key step and many efforts have been paid to develop new irradiation setup and materials compatible with sub-100 nm resolution. Among other resist platforms, chemically amplified photoresists (CAR) are widely used because of their excellent properties in terms of resolution, sensitivity, and etching resistance. However, low information on the impact of the polymer structure on the lithography performance is available. CAR with well-controlled polymer structures were thus prepared and investigated. In particular, the impact of the polymer structure on the lithographic performance was evaluated. Linear

and branched polymers with various molecular weights and polydispersities were compared. We focused on the dependency of the photosensitivity of the resist with the structural parameters. These results allow further understanding the fundamental phenomena involved by 193-nm irradiation.

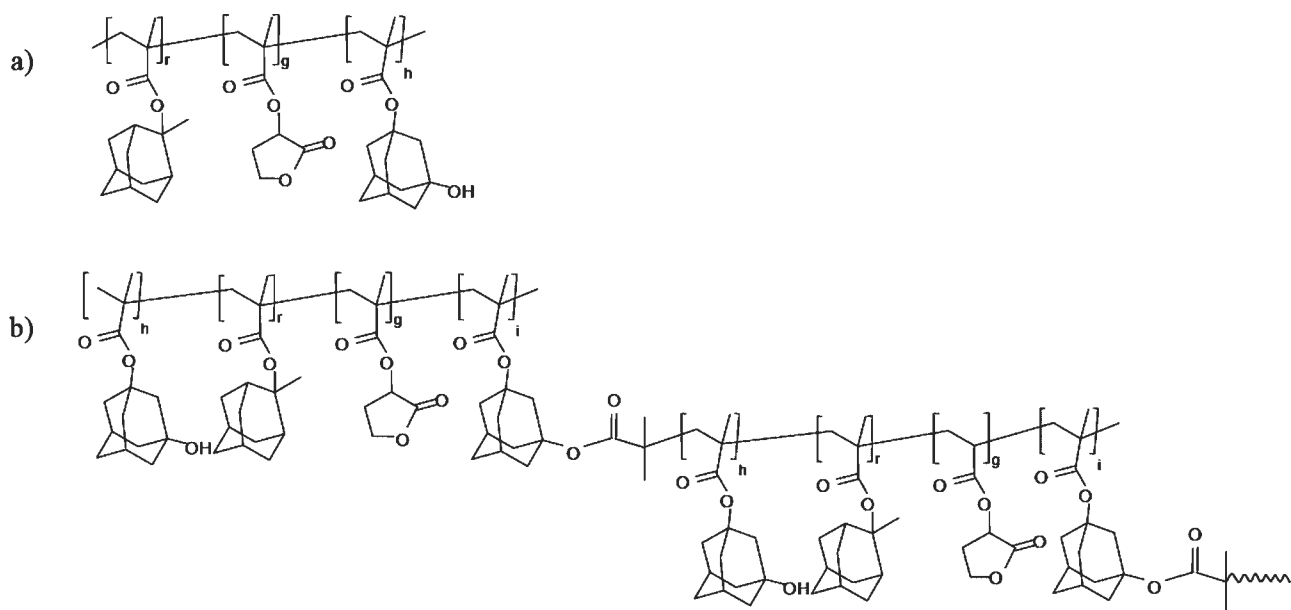
KEYWORDS: atomic force microscopy; atom transfer radical polymerization; chemically amplified photoresists; hyper-branched polymer; nanotechnology; photolithography; photoresists; resists

INTRODUCTION Deep UV (DUV) photolithography has become the current technique used in the industry of microelectronics for production of submicron structures. Chemically amplified photoresists (CAR) are the predominant materials used in the fabrication of nanoscale structures with 193-nm photolithography.¹ Patterns are defined chemically through the production of acid in areas exposed to DUV light and an acid-catalyzed deprotection reaction that changes the solubility of the reacted material in an aqueous base solution.² The patterning process is complex because many composition and process parameters have an impact on the photolithographic performances of the photoresist. Among these parameters, those linked to the resist materials are considered as the most critical. Three factors are essential to consider: resolution limit, sensitivity, and line width roughness (LWR). Resolution limit is the most important criterion because the new platforms of resists should be able to address the challenging next lithographic nodes under 45 nm. However, sensitivity is a parameter of importance for practical applications due to the necessity to achieve short exposure times. LWR and line edge roughness (LER), measuring the deviation from an atomically smooth surface

have become new parameters preventing the feasibility of smaller feature sizes.³ LWR and LER are mainly attributed to the chemistry and the properties of the photoresist polymer.^{2,4} However, other parameters like the nature and concentration of photoacid generator (PAG),⁵ the base quencher or other additives,⁶ and almost all the intermediate process steps have been recognized to play a role on the final LWR and LER, such as exposure,⁷ postexposure baking (PEB),⁸ and development.⁹ Lot of research efforts have been deployed for optimizing each step of the lithographic processing or for stabilizing the PAG phase separation and the photoacid distribution,¹⁰ nonetheless, LER and LWR values remain still high.

The nature of the polymer significantly contributes to all aspects of resist characteristics and performance. Most of the polymers used as resists are linear copolymers or terpolymers synthesized by the free radical polymerization technique.^{2,11} Such technique has the advantage to be relatively simple but the main drawback is a limited control of the polymer chain structure.

Advanced polymer synthesis strategies like atom transfer radical polymerization (ATRP) were recently proposed to



SCHEME 1 Molecular structures of the copolymers used in the DUV resists. (a) Linear polymer and (b) hyperbranched polymer. r , g , and h were, respectively, 30%, 50%, and 20%. The relative proportion of the monomer in the terpolymer is designed by the parameters (r , g , h), corresponding, respectively, to *R*-AMA, GBLMA, and HAdMA monomers.

achieve a better control of the polymer structure, with both linear and hyperbranched structure and for a large variety of monomers.¹²

The aim of this work is to compare the photosensitivity of resists comprising polymers with various well-defined structures. Linear polymers were first investigated. The impact of the polymer molecular weight, the chemical composition of the polymer, and its polydispersity were investigated. Different process parameters were also adapted regarding the polymer composition.

The study was extended to innovative hyperbranched polymers. Such a structure was recently proposed for 193-nm lithography.¹³ The molecular compact structure is supposed to allow decreasing the LER. We have studied here the response of this hyperbranched polymer and compared it with linear polymers in terms of response to process and photonic parameters.

EXPERIMENTAL

Chemicals

Linear and branched terpolymers were synthesized by ATRP. The hyperbranched polymers were synthesized using the self-condensing vinyl polymerization strategy developed by Fréchet et al.¹⁴ The details of polymer synthesis and polymer structure characterization are given in ref. 13. The structures of both linear and branched polymers are given in Scheme 1. The three monomers used to prepare the terpolymer are methyl adamantyl methacrylate (*R*-AMA), α - γ butyrolactone methacrylate (GBLMA), and hydroxyl functionalized adamantyl methacrylate (HAdMA). The three monomers composing the final structure of the copolymer are related to a specific property for the use of the resist in a microelectronics con-

text (etching resistivity, adhesion, and deprotection). The relative proportion of the monomer in the terpolymer is designed by the parameters (r , g , h), corresponding, respectively, to *R*-AMA, GBLMA, and HAdMA.

The polymers were dissolved in cyclohexanone (99.8%; Aldrich). Triphenylsulfonium perfluorobutyl sulfonic acid of 3 wt % (99+%; Aldrich) was added as a PAG and 0.2 wt % of trioctyl amine (98%; Aldrich) as a quencher. After stirring for a few hours, the solutions were filtered with a 0.2 μm Teflon filter.

All resists were deposited on single-crystal undoped Si (100) wafer polished on one side by spin-coating. A bottom antireflective coating layer (BARC) was systematically deposited on the Si substrate before the resist deposition to decrease the back reflection on Si and also to improve the adhesion of the resist on the substrate. The targeted resist thickness was 120 nm. The spinning rate was adjusted to achieve this thickness.

Nanopatterning Process

After spin-coating deposition, the films were heated on a hotplate to remove the residual solvent and densify the polymer layer Post-Apply Bake (PAB). The photosensitive resist was then exposed with different light doses to generate the acid production in the irradiated part.

Patterns were generated by irradiation using an ArF excimer laser equipped with an interferometric setup.¹⁵ The interferometer comprises phase masks specially designed to eliminate the zeroth diffraction order. The phase masks were irradiated in normal incidence. The ± 1 diffraction orders generated by the phase mask recombined within the polymer films, creating a sinusoidal distribution of light that was used to induce the surface patterning of the film. Typically,

the irradiated surface was $8 \text{ mm} \times 4 \text{ mm}$, with good homogeneity (5% in intensity). The pitch could be tuned between 150 nm and 500 nm. In the present study, patterns with a period of 200 nm were fabricated.

After laser irradiation, a Post-Exposure Bake (PEB) was applied for varying time and temperature to induce the deprotection of the resist. After baking, the samples were developed by immersion in 0.26 N tetramethylammonium hydroxide (TMAH) for 60 s and rinsed with deionized water.

Pattern images were characterized by Atomic Force Microscopy (AFM), in resonant mode using a PicoPlus commercial microscope (Molecular Imaging). Noncontact high frequency Silicon tips ($C = 42 \text{ N/m}$, $f_0 = 285 \text{ kHz}$) were used. Two-dimensional cross-section profiles were extracted to characterize the depth of the lines written by 193-nm lithography. Scanning electronic microscopy (SEM) was used to visualize the nanostructures.

RESULTS AND DISCUSSION

Linear Polymers—Impact of the Molecular Weight and Polydispersity

The patterning performance of the resist is a complex result of parameters linked to the resist formulation and the process parameters. Among the different components of the resist, the polymer matrix is probably the most important. However, only few works report the impact of the polymer matrix on the resist performance on an equivalent polymer platform.^{11,16} One of the difficulties is linked to their complex polymer synthesis with controlled and well-defined molecular properties in a wide range of compositions. To state the role of molecular weight, composition, and polydispersity of a terpolymer on the photolithographic performances, various polymer samples were prepared and the corresponding resists were tested.

Figure 1 is aimed at illustrating typical profiles of patterns that were obtained by DUV interferometry. The SEM image on Figure 1(a) is relative to a polymer suitable for nanopatterning ($M_n = 5.000 \text{ g/mol}$; $\text{PDI} = 2$). As it can be observed, the patterns are well-defined, with steep edges and low rugosity. Such profiles are required because they will provide a transfer into the silicon substrate with high fidelity and ensure *in fine* an optimum performance of the electronics device. On the contrary, Figure 1(b) illustrates the best profile obtained with a second polymer ($M_n = 130.000 \text{ g/mol}$; $\text{PDI} = 6$) under the same curing conditions ($T_{\text{PAB}} = T_{\text{PEB}} = 115 \text{ }^\circ\text{C}$). In this case, the maximum depth of the profiles was in the range of a few nanometers. For lower dose, no activation of the resist was observed. When the dose was increased, the resist was deprotected within the whole exposed volume and thus it was fully solubilized after development. Such behavior is characteristic of a low resolution resist which is incompatible with nanoscale patterning.

To further exemplify the differences due to the polymer structure, the optimum dose window was determined for several polymers with M_n ranging between 5.000 and 130.000 g/mol. The results are presented in Figure 2. For

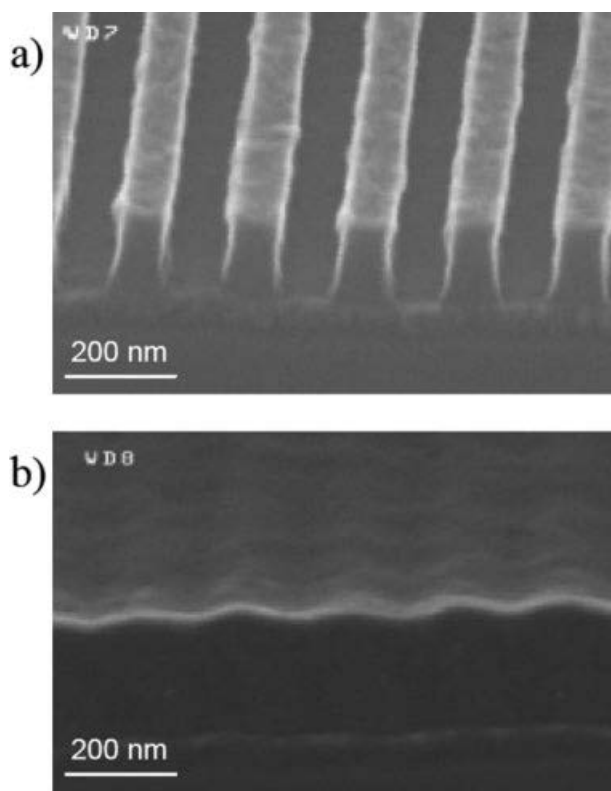


FIGURE 1 SEM images of typical patterns obtained by DUV interferometry. (a) Polymer exhibiting good lithographic performances ($M_n = 5.000 \text{ g/mol}$; $\text{PDI} = 2$), giving rise to a structure with a binary type profile. (b) Low resolution polymer ($M_n = 130.000 \text{ g/mol}$; $\text{PDI} = 6$) for which no suitable pattern could be obtained at any dose for the curing conditions chosen ($T_{\text{PAB}} = T_{\text{PEB}} = 115 \text{ }^\circ\text{C}$).

each polymer, three values of the dose have been plotted: the minimum dose for which patterns started to be obtained (lower line), the optimum dose (dot), and the maximum dose before overexposure (upper line). The difference between the extreme values gives the exposure latitude of the resist. If the exposure latitude is low, the correct dose will be difficult to define and a slight modification of the environmental parameters may deteriorate dramatically the pattern profile. High-exposure latitude will facilitate the DUV patterning process. This characteristic is thus of high importance for practical applications of the photoresist.

It has to be emphasized that the same curing temperatures (T_{PAB} and T_{PEB}) were chosen for this family of polymers. Indeed, the T_g of these polymers were determined and were found to be almost independent on the molecular weight between 25.000 and 130.000 g/mol. Only the polymers with lowest molecular weights were found with significantly lower T_g . All values can be found in Table 1.

Polymers A, B, C, and D have all the same composition: they are copolymers comprising the 3 different monomers (*R*-AMA, GBLMA, and HAdMA) with the same relative feed proportion ($r = 30\%$, $g = 50\%$, $h = 20\%$, respectively) and same PDI. Complete patterning (down to the substrate)

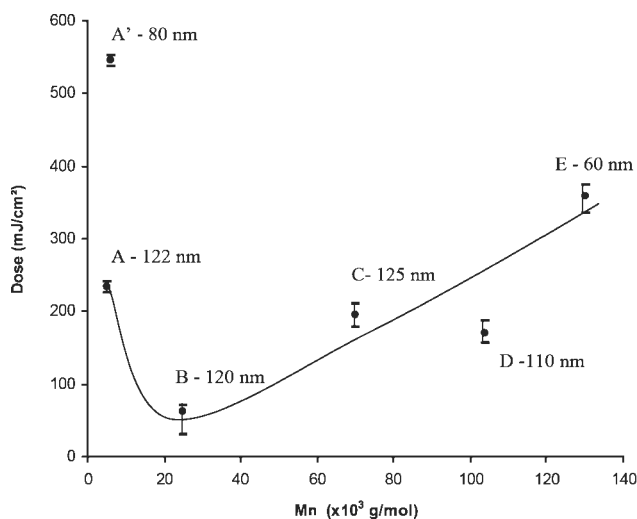


FIGURE 2 Influence of the molecular weight of the linear polymer on the dose needed to generate patterns. The error bars symbolize the exposure latitude (corresponding to the lower and higher doses for which patterns were obtained). The center dot is the optimal dose, defined as the dose that gives rise to the maximum relief amplitude (maximal value in nanometer given in the figure for each polymer). Polymers A, B, C, and D had all the same molecular composition ($r = 30\%$, $g = 50\%$, $h = 20\%$) and same PDI. Polymer E has the same composition but a PDI = 6. Polymer A' had the following composition: ($r = 60\%$, $g = 25\%$, $h = 15\%$). $T_{\text{PAB}} = 115\text{ }^{\circ}\text{C}$, $T_{\text{PEB}} = 115\text{ }^{\circ}\text{C}$. Line is aimed at guiding eye.

could be achieved only for polymers with molecular weight inferior to 70.000 g/mol. Differences observed between maximum relief amplitude results from the dispersion in initial film thickness. For 104.000 g/mol, a complete patterning could not be obtained though the relief amplitude is close to the initial resist thickness. In this case, the profile at the optimum dose was not as exposed in Figure 1(a) but it was sinusoidal. As it can be seen in Figure 2, the exposure latitude is almost independent on the molecular weight. Only the resist with the lowest molecular weight polymer corresponded to low-exposure latitude.

Interestingly, all polymer films exhibit sensitivity in the same order of magnitude. The smaller chain (A: 5.000 g/mol) needed a slightly higher dose to be activated. Such behavior can be related to the higher compaction occurring within this film during PAB due to lower T_g . The consequence is then a lower diffusion of the acid after exposure.

The polymer E was chosen with the same composition as that of polymer D but with a higher PDI (PDI = 6). In this case, a higher dose was needed to obtain patterns. Such behavior may have two origins: first, the compaction during PAB is favored by the high polydispersity, and second, long polymer chains are more difficult to extract during development. Thus, the modification of a higher proportion of functional groups is necessary to ensure the solubility of the irradiated parts of the film. Moreover, with these process parameters, such resist could not be efficiently patterned

since the maximum relief amplitude remained inferior to 60 nm.

The impact of the proportion of acid-cleavable monomer was also evaluated (*R*-AMA). Polymer A' was chosen with a molecular weight in the same order of magnitude as polymer A but with a different composition: ($r = 60\%$, $g = 25\%$, $h = 15\%$). Compared with the other polymers, the proportion of photoactivable monomer (r) is thus higher from a factor of 2. Interestingly, the dose needed to obtain patterns was found twice greater than for the reference composition. This result illustrates the direct correlation between the concentration of the *R*-AMA monomer and the sensitivity of the resist.

From these first results, it can be deduced that the molecular weight has a relatively low impact on the sensitivity. The sensitivity is mostly governed by the proportion of activable monomer. Low-molecular weight polymers are more suitable for a complete lithography.

Linear Polymers—Impact of the Process Parameters

Further investigation on the highest molecular weight polymer was carried out to understand the impact of the process parameter for such polymer architecture (namely, PAB and PEB). Indeed (115/115 °C) was chosen with regards to the smaller molecular weight resists and such conditions may not be relevant for the highest polymer molecular weights (130.000 g/mol). The impact of an increase of the (PAB, PEB) temperatures is shown on Figure 3. In this case, the resists prepared with the 104.000 and 130.000 g/mol polymer were evaluated with (PAB-PEB) temperatures increased up to (120/120 °C).

For both polymers, higher curing temperatures had a negative impact on both patterning capacities and photosensitivity of the resist. Indeed, for the 104.000 g/mol polymer, the maximum relief modulation achievable was decreased from 110 nm (which corresponds to the nominal thickness of the resist film) to 75 nm. Thus, the resist that could be fully patterned at (115/115 °C) could no longer be patterned at (120/120 °C). In parallel the dose needed to obtain the

TABLE 1 Structure and T_g of the Polymers Used in this Study

Polymer	Structure	M_n (g/mol)	PDI	T_g (°C)
A	Linear	5.000	2	129
A'	Linear	6.600	2.5	134
B	Linear	25.500	1.8	180
C	Linear	70.000	2	185
D	Linear	104.000	2	195
E	Linear	130.000	6	190
H1	Hyperbranched	10.600	1.4	170
H2	Hyperbranched	11.800	1.7	181
H3	Hyperbranched	13.000	1.6	180
H4	Hyperbranched	13.200	2.5	185

M_n and PDI determined by SEC (PMMA standard) and T_g evaluated by DSC.

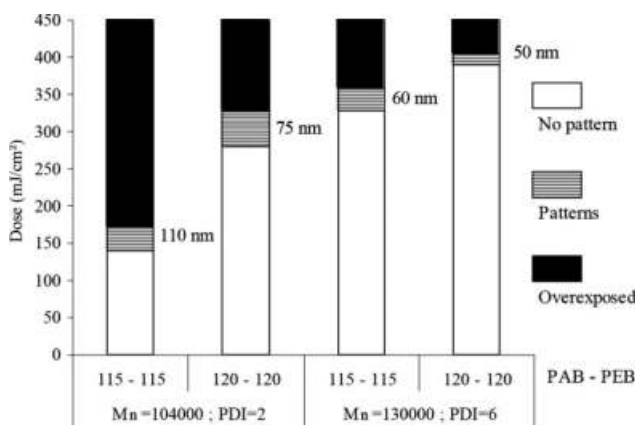


FIGURE 3 Impact of the polydispersity and curing temperature (PAB and PEB) on the needed dose to pattern the resist. The limits of the gray box (patterns) correspond to the exposure latitude. The value in nanometer given in the graph corresponds to the maximum relief amplitude measured by AFM.

maximum relief amplitude increased by a factor of 2 by changing the curing temperatures. For the resist comprising the 130.000 g/mol polymer, the increase of the curing temperature had also a negative influence, in terms of patterning and photosensitivity, confirming the same trend as exposed previously.

Such behavior demonstrates a prominent impact of the PAB. Indeed, an increase of the PEB generally results in a decrease of the needed dose since the deprotection reaction is favored at high temperature. On the contrary, an increase of the PAB temperature requires a higher dose because of the further densification of the resist. In the present case, the result of these two contradictory phenomena demonstrates that the effect on the PAB govern the temperature dependency of the resist. This parameter needs thus to be adjusted with maximum care.

The effect of thermal curing parameters was also investigated more extensively for the 70.000 g/mol polymer (Fig. 4). The reference conditions (115 °C, 115 °C) gave rise to a maximum patterning capacity (maximum height = 125 nm). When the PAB was increased to 120 °C with the same PEB temperature (115 °C), no pattern could be obtained. The dose at which the polymer film started to be modified is slightly increased but the main effect is the complete loss of the exposure latitude. The further compaction of the polymer induced by a higher PAB temperature probably accounts for this behavior. The importance of PAB on lithographic performances is emphasized, like in previous example. For such a PAB temperature, it is however possible to pattern the polymer if a higher PEB temperature is used (120 °C). In this case, patterns were obtained in a wide range of dose, which remained always lower than the reference conditions. However, these experimental conditions revealed to be unsuitable for patterning since the maximum relief amplitude was inferior to 10 nm.

Lower PAB led to a significant decrease of the needed dose. For a PAB of 100 °C, patterns were obtained at 30 mJ/cm².

In this case, the maximum relief amplitude was 85 nm. Once again, these conditions did not allow a complete patterning and thus they are not interesting for practical applications.

These results stress out that the process parameters significantly affect the patterning potential of the resist. Moreover, it was demonstrated that the PAB temperature dramatically influences the photosensitivity of the resist and this parameter has to be adjusted with care when varying the molecular parameters of the polymer.

Hyperbranched Polymer—Impact of Polymer Structure

The use of another type of polymer architecture for formulation of a 193-nm CAR photoresist was recently proposed.¹³ It relies on an innovative hyperbranched copolymer matrix. For branched systems with high density of sterically congested peripheral groups, one can expect a smaller radius of gyration, compared with linear polymers, and thus a significant decrease of LER and LWR. The first results demonstrating the potential of such polymer structure for 193-nm photolithography were presented in ref. 13. We present here the response of resists based on this hyperbranched polymer toward photonic parameters to further describe the impact of the polymer structure on the photolithographic properties.

Figure 5 presents a typical SEM of the nanostructures obtained by DUV interferometry. Patterns with a width of 100 nm could be obtained. The LER(3 σ) was evaluated to be 6 nm using 3D-AFM. This value is in the range of commercially available 193-nm resists.

Figure 6 illustrates the dependency of the relief amplitude for increasing doses. The relief amplitude was evaluated using AFM in resonant mode. The half-pitch was 100 nm insuring that the AFM tip could effectively enter inside the patterns. No pattern was obtained for a dose lower than 30 mJ/cm². Interestingly, this value is much lower than the values presented for linear polymers. It has to be emphasized that the resists with the hyperbranched polymers contained 5 wt % PAG, whereas the linear polymers contained only 3 wt %. Resists with hyperbranched polymers doped with 3 wt % PAG

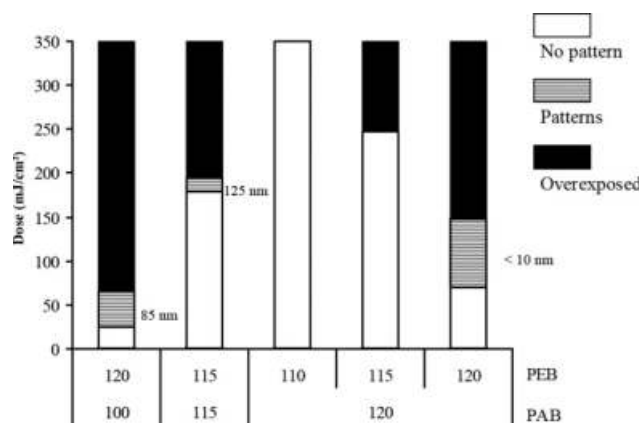


FIGURE 4 Impact of the curing temperature (PAB and PEB) on the needed dose to pattern the resist composed of the polymer ($M_n = 70,000$ g/mol; PDI = 2).

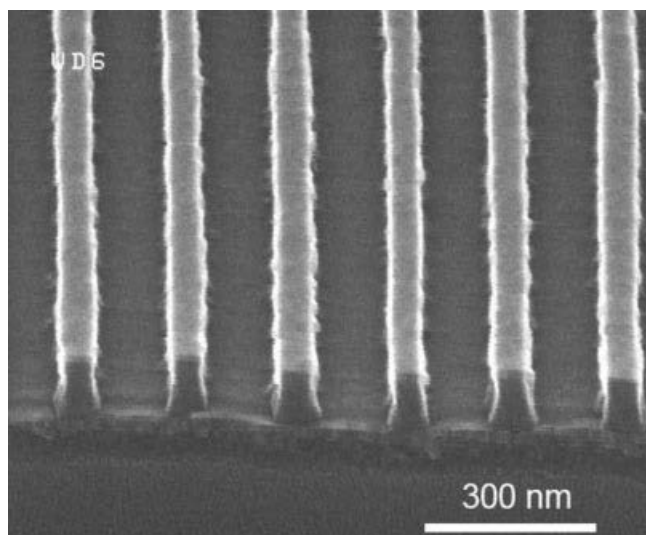


FIGURE 5 SEM images of patterns obtained by DUV interferometry with the hyperbranched polymer (200 nm pitch).

exhibited almost no photosensitivity for doses inferior to 300 mJ/cm^2 . The addition of 2 wt % PAG allowed significantly decreasing the dose needed to activate the resist. Such difference between linear and hyperbranched polymer can be possibly attributed to the impact of basic residue of the polymer synthesis remaining in the final product, even after several appropriate purification steps: the polymers were synthesized in clean room with electronics grade solvents and precipitated in MeOH. All the glasses were washed in electronic grade solvents as well. Using these conditions, the contamination of polymers by metals was reduced under 10 ppm for most metals. Only Sodium and Calcium (23 and 11 ppm, respectively) were significantly above. Further efforts will be made in the next future to decrease the residual metal contamination. However, the hyperbranched polymers were tested regarding their lithographic capacities. Maximum relief amplitude was obtained for 93 mJ/cm^2 . The height of the structures corresponded to the initial value of the resist films, which means

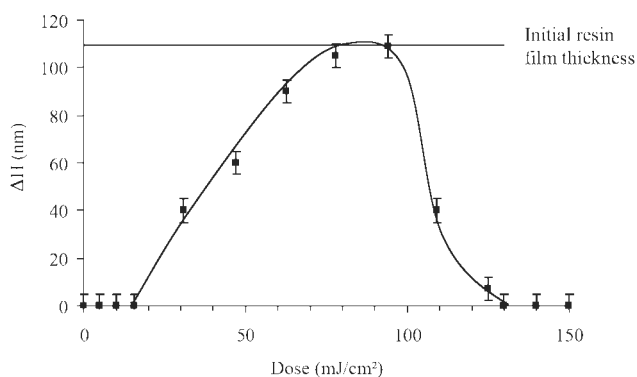


FIGURE 6 Response of a resist comprising a hyperbranched polymer with incident dose. The evolution of the relief amplitude within the grating was evaluated by AFM and plotted. The pitch was 200 nm. The polymer had a molecular weight of 13.200 g/mol.

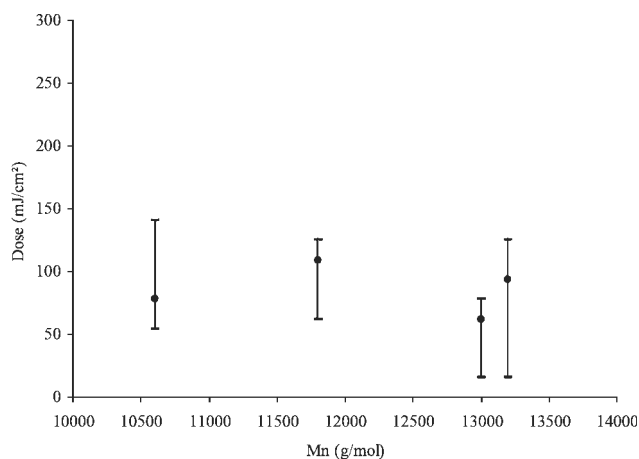


FIGURE 7 Influence of the molecular weight of the hyperbranched polymers on the dose needed to generate patterns. The error bars symbolize the dose range for which patterns were obtained. The dot is the optimal dose, defined as the dose that gives rise to the maximum relief amplitude.

that the resist film was effectively patterned through the whole thickness of the photoresist. The dose latitude is relatively low because the grating was completely erased for the optimum dose +20%. After 130 mJ/cm^2 , the resist was completely removed after development. The sensitivity of this new resist is thus in the same order as the linear polymer-based resists. Moreover, the LER and resolution that were obtained demonstrate that it can be an excellent candidate for the next generation of 193-nm CAR.

The reactivity of several resists with hyperbranched polymers with different molecular weights was evaluated (Fig. 7). Because of the synthesis limitation, the range of M_n was relatively low but it corresponds to molecular weight of highest interest (low-molecular weight). Considering the T_g of these polymers (cf. Table 1), the curing conditions were kept at the same values as for linear polymers ($T_{PEB} = T_{PAB} = 115^\circ\text{C}$). For all samples, the maximum relief amplitude obtained corresponded to the initial film thickness, demonstrating that all hyperbranched polymer-based resists could be successfully patterned. All resists exhibited a photosensitivity in the same order of magnitude. In particular, no effect of the branching density or of the monomer relative proportion could be detected.

The photolithography properties of these new resists fulfill the requirements for practical applications, in term of sensitivity, resolution and LER. Further optimization of the process parameters is under development to fully use the potential of this polymer architecture. The resistance of these resists to dry etching is under evaluation. It is supposed to be as resistant as the linear resists since the chemical nature of the monomers that compose the material are the same.

CONCLUSIONS

The impact of the composition and process parameters on the photolithographic performance of chemically amplified

resists was reported. The preparation of various terpolymers with well-defined and controlled molecular structure allowed evaluating the influence of the polymer structure on the photosensitivity of the resist. We demonstrated the interest of low-molecular weight polymer and the importance of the curing parameters on the resulting nanostructures. The potential of a new class of terpolymers with hyperbranched structure was also discussed. It was shown that the photolithographic performances of such resists are comparable with linear resists. Thus, they appear as potential candidates for the next generations of chemically amplified resists.

The authors gratefully thank *Agence National pour la Recherche* (ANR) for financial support (Program PNANO ANR-05-NANO-056, NANORUGO) and *Rohm and Haas Electronic Materials* (D. Perret and C. Brault) for providing monomers and resists and for fruitful discussions.

REFERENCES AND NOTES

- 1 (a) Bowden, M. J.; Turner, S. R. *Electronic and Photonic Applications of Polymers, Advances in Chemistry*, Eds Bowden, M. J.; Turner, S. R., Washington, 218, 1988; (b) Macdonald, S. A.; Wilson, C. G.; Fréchet, J. H. J. *Acc Chem Res* 1994, 27, 151–158.
- 2 Ito, H. *Adv Polym Sci* 2005, 172, 37–245.
- 3 Yoshimura, T.; Shiraishi, H.; Yamamoto, J.; Okazaki, S. *Jpn J Appl Phys* 1993, 32, 6065–6070.
- 4 (a) Cutler, C. A.; Mackevich, J. F.; Li, J.; O'Connell, D. J.; Cardinale, G.; Brainard, R. L. *Proc SPIE* 2003, 5037, 406–417; (b) Kim, J.-B.; Kim, K.-S. *Macrom Rapid Commun* 2005, 26, 1412–1417; (c) Ogata, T.; Matsumaru, S.; Shimizu, H.; Kubota, N.; Hada, H. *J Photopolym Sci Technol* 2004, 17, 483–488.
- 5 (a) Wallraff, G. M.; Larson, C. E.; Fender, N.; Davis, B.; Medeiros, D.; Meute, J.; Lamanna, W. M.; Parent, M. J.; Robledo, T.; Young, G. *Proc SPIE* 2002, 4690, 160–168; (b) Yoshizawa, M.; Moriya, S. *J Vac Sci Technol B* 2002, 20, 1342–1347; (c) Kim, J.-H.; Kim, Y.-H.; Chon, S.-M.; Nagai, T.; Noda, M.; Yamaguchi, Y.; Makita, Y.; Nemoto, H. *J Photopolym Sci Technol* 2004, 17, 379–384; (d) Schmid, G. M.; Stewart, M. D.; Singh, V. K.; Willson, C. G. *J Vac Sci Technol B* 2002, 20, 185–190.
- 6 (a) Shiobara, E.; Kawamura, D.; Matsunaga, K.; Koibe, T.; Mimotogi, S.; Azuma, T.; Onishi, Y. *Proc SPIE* 1998, 3333, 313–323; (b) Michaelson, T. B.; Jamieson, A. T.; Pawloski, A. R.; Beyers, J.; Acheta, A.; Wilson, C. G. *Proc SPIE*, 2004, 5376, 1282–1300.
- 7 (a) Hinsberg, W.; Houle, F. A.; Hoffnagle, J.; Sanchez, M.; Wallraff, G.; Morrison, M.; Frank, S. *J Vac Sci Technol B* 1998, 16, 3689–3694; (b) Pawloski, A.; Acheta, A.; Levinson, H.; Michaelson, T. B.; Jamieson, A. Nishimura, Y.; Willson, C. G. *J Microlith Microfab Microsyst* 2006, 5, 023001–17; (c) Shin, J.; Han, G.; Ma, Y.; Moloni, K.; Cerrina, F. *J Vac Sci Technol B* 2001, 19, 2890–2895.
- 8 (a) Reynolds, G. W.; Taylor, J. W. *J Vac Sci Technol B* 1999, 17, 334–344; (b) Shin, J.; Ma, Y.; Cerrina, F. *J Vac Sci Technol B* 2002, 20, 2927–2931.
- 9 (a) Houle, F. A.; Hinsberg, W. D.; Sanchez, M. I. *Macromolecules* 2002, 35, 8591–8600; (b) Tsiartas, P. C.; Flanagan, L. W.; Henderson, C. L.; Hinsberg, W. D.; Sanchez, I. C.; Bonnacaze, R. T.; Willson, C. G. *Macromolecules* 1997, 30, 4656–4664.
- 10 (a) Dumond, J.; Low, H. Y. *Adv Mater* 2008, 20, 1291–1297; (b) Wang, M.; Jarnagin, N. D.; Lee, C.-T.; Henderson, C. L.; Yueh, W.; Roberts, J. M.; Gonsalves, K. E. *J Mater Chem* 2006, 16, 3701–3707; (c) Wang, M.; Yueh, W.; Gonsalves, K. E. *Macromolecules* 2007, 40, 8220–8224.
- 11 Kang, S. H.; Prabhu, V. M.; Vogt, B. D.; Lin, E. K.; Wu, W.-L.; Turnquest, K. *Polymer* 2006, 47, 6293–6302.
- 12 (a) Xia, J.; Matyjaszewski, K. *Chem Rev* 2001, 101, 2921–2990; (b) Kamigaito, M.; Ando, T.; Sawamoto, M. *Chem Rev* 2001, 101, 3689–3746.
- 13 Chochos, C. L.; Ismailova, E. S.; Brochon, C.; Leclerc, N.; Tiron, R. A.; Sourd, C.; Bandelier, P.; Foucher, J.; Ridaoui, H.; Dirani, A.; Soppera, O.; Perret, D.; Brault, C.; Serra, C. A.; Hadziioannou, G. *Adv Mater* 2009, 21, 1121–1125.
- 14 Fréchet, J. M. J.; Hemmi, M.; Gitsov, I.; Aoshima, S.; Leduc, M. R.; Grubbs, R. B. *Science* 1995, 269, 1080–1083.
- 15 Soppera, O.; Dirani, A.; Ponche, A.; Roucoules, V. *Nanotechnology* 2008, 19, 395304 (9pp).
- 16 (a) Okoroanyanwu, U.; Byers, J.; Shimokawa, T.; Willson, C. G. *Chem Mater* 1998, 10, 3328–3333; (b) Houlihan, F. M.; Walllow, T. I.; Nalamasu, O.; Reichmanis, E. *Macromolecules* 1997, 30, 6517–6524.